The 2nd International Symposium on Thermal Stresses and Related Topics, Rochester Institute of Technology, Rochester, NY, June 8-11, 1997

SAND--97-8555C
CONF-9706191--

Finite Element Modeling of Weld Solidification Cracking in 6061-T6 Aluminum - Applicability of Strain-based Failure Criteria

J. J. Dike*, J. A. Brooks, D. J. Bammann*, M. Li****

**Mechanics & Simulation of Manufacturing Processes Department,*
***Advanced Manufacturing Technologies for Metals Processing Department,*
Sandia National Laboratories, Livermore, CA, 94550

Finite element simulations using an internal state variable constitutive model are used to study weld solidification cracking of 6061-T6 aluminum. Stress and strain histories at the weld centerline for two types of specimen are studied with regards to application of strain-based failure criteria for predicting weld solidification cracking.

Key Words: Solidification Cracking, Welding Strains, Aluminum, Thermal Stresses, Welding Stresses

1. Introduction

Weld solidification cracking has been observed experimentally for more than fifty years. Finite element simulations of weld solidification cracking are much more recent [1-7]. The metallurgical aspects of solidification cracking have been studied in much more detail than the thermomechanical aspects and the interaction between them is not yet well understood.

Many theories have been presented aiming at the capability of predicting weld solidification cracking. References [1] and [8] present overviews of several theories. Some do not include a consideration of the mechanical loads while others do not consider microstructural aspects. Some theories focus on strains as the critical factor in determining if cracking occurs, while others focus on stresses.

In this work we present calculations of stresses and strains in two types of specimens. Calculated strains at crack initiation sites are compared for different weld parameters with respect to strain-based failure criteria.

2. Experiments

The experiments are discussed in detail in [7]. Briefly, two types of 6061-T6 aluminum specimens, 6.35 mm thick with 1.27 mm thickness in the welded regions, were used to study solidification cracking. One type of specimen was a 101.6 mm diameter disk shown schematically in Figure 1. Table 1 lists parameters for two test welds. Figure 2 shows the second type of specimen with dimensions of 76.2 mm x 152.4 mm. Welds were made using 55 A and 70 A currents and 12.7 mm/s travel speeds. All welds were made using the gas tungsten arc process with a voltage of 17 V.

Table 1. Weld process parameters for disk tests.

Test	current (A) location from weld start 0-120°	120-240°	240-360°	weld travel speed (mm/s)
1	50	55	60	6.35
2	30	40	50	6.35

3. Thermal Finite Element Analyses

A solidification model incorporating both dendrite tip and eutectic undercooling was used. Reference [7] provides details about the 3D thermal analyses.

Information from the solidification model was used in the thermal analyses to modify the temperature dependent specific heat. Calculations were verified using thermocouples, fusion zone cross-sections, and weld pool ripple shapes.

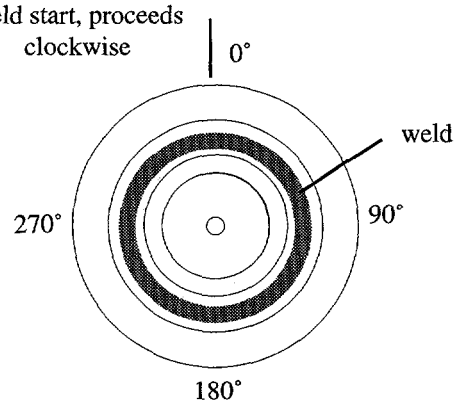

Figure 1. Schematic of weld on disk specimen showing location of weld and locations of elements used to study stresses and strains.

DISCLAIMER

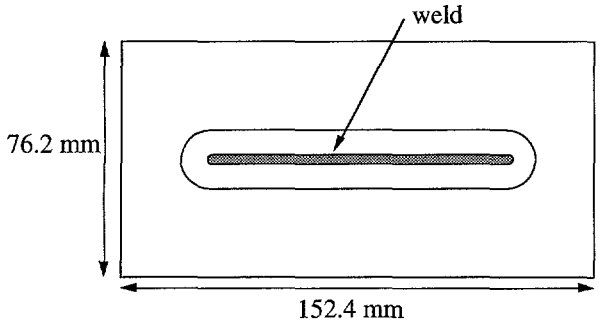

Figure 2. Schematic of rectangular specimen used to verify calculations of temperatures and average strains across the weld.

4. Mechanical Finite Element Analyses

A strain rate and temperature history dependent internal state variable constitutive model [9] was used in the 3D mechanical analyses. The thermal expansion strain increased nearly linearly with temperature to 1.85% at the solidus temperature of 828 °K. The slope of the thermal expansion strain was increased throughout the solidification range of 828 °K to 928 °K to account for an additional 2.2% of expansion strain due to the liquid-solid phase transition [1]. The strain was distributed at a rate dictated by the solidification model's prediction of fraction solid as a function of temperature. Additional details may be found in [7].

5. Strains in the Weld

Video techniques were developed to measure strains as the weld approached and traversed specific regions of the weld. Comparisons of calculated and measured strain histories averaged across the weld for Houldcroft specimens and the rectangular specimens discussed here have been presented in [5] and [7] respectively. The gage length over which the strains were measured was approximately 6.35 mm for both cases. These comparisons provided some confidence that the techniques and properties used in the simulations were useful in providing good estimates of the mechanical responses for specimens that did not crack. We now present calculated strains along the weld centerline to study the applicability of strain-based failure criteria for solidification cracking.

5.1 DISK SPECIMENS

Figure 1 shows the locations of elements used to study the stress and strain histories for the disks. The elements of interest are located at the weld centerline at 0°, 90°, 180°, and 270° from the weld start. Figure 3 shows histories of total strains for four elements located along the length of a weld for a simulation of Test 1 in Table 1. In Test 1, the specimen cracked very close to the weld start. Failure was not allowed in the calculation so that the strain at various crack initiation points could be determined. It is interesting to note that neither the peak nor the final strains increase monotonically with position along the weld for this set of weld parameters. More importantly, the recovery strains, which arise as the material experiences a tensile stress, do increase with distance from the weld start. This is consistent with observed cracking trends. All locations experience very similar histories, with final strains between 2% and 4%, similar in magnitude to strains averaged across the welds in previous comparisons [5,7]. However, strain histories averaged across the welds do not show the large dips observed both in simulations and experiments at the centerline.

The large dips observed are associated with the passing of the weld pool. Figure 4 shows the transverse strain history of the element at 90° for the simulation of disk Test 1 relative to the temperature and transverse stress histories. The curves show that the dip in strain begins very near when the temperature reaches the liquidus temperature (928 °K). The bottom of the dip occurs before the tail of the weld pool (liquidus temperature) passes the element. The strain does not level off until approximately 100 °K below the solidus temperature of ~ 828 °K.

The response can be explained by examining the transverse stress history relative to the strain history. A large compressive stress is observed just prior to the arrival of the weld pool. When the weld pool reaches the element, the stress becomes close to zero until after the weld pool passes. The large increase in shrinkage (strain) occurs when the weld pool is passing the element. The response can be thought of as the material being in compression, then having a "hole" form by the passing weld

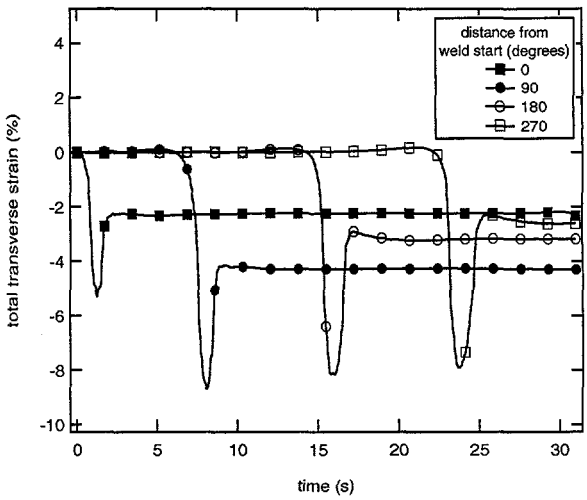

Figure 3. Total transverse strains for elements along disk weld centerline for simulation of Test 1 in Table1.

pool which allows a large contraction in the material due to the preexisting compressive load. The leveling off of the strain corresponds to the passing of the weld pool and the development of a tensile stress at that point.

Figure 5 presents total transverse strain histories for disk weld Test 2 in Table 1. The specimen cracked at approximately 190° from the weld start in this test. Again, no damage was allowed to accumulate in the simulation. Figure 5 shows a response similar to that in

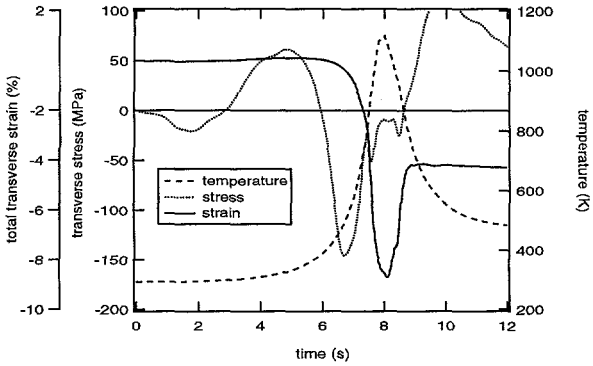

Figure 4. Transverse stress and strain and temperature for centerline element at 90° in simulation of disk weld Test 1.

Figure 3 for Test 1. However, the magnitudes of the peak strains are a few percent smaller and the peak strains do increase monotonically.

5.2 RECTANGULAR SPECIMENS

The strain response calculated for the rectangular specimens is quite similar to that calculated for the disks. Figure 6 shows the total transverse strain histories for a 70 A, 17 V, 12.7 mm/s GTA weld on a rectangular specimen. The elements are located on the centerline near the weld start, halfway along the weld, and near the end of the weld. Damage accumulation was turned off in this analysis. Another simulation at 55 A shows the same trend with peak strains approximately 2% larger for the 70 A weld. Final strains (at 8 s, when the arc is turned off) were nearly identical for both analyses, with ~2% and ~5% at the start and midpoint of the welds, respectively.

5.3 MECHANICAL STRAINS

Mechanical strains are often used in strain-based solidification cracking failure criteria. The mechanical strain is defined here as the total strain less the thermal strain referenced from the liquidus temperature. It represents the mechanical strain accumulated during solidification.

Matsuda and coworkers [10,11] studied mechanical

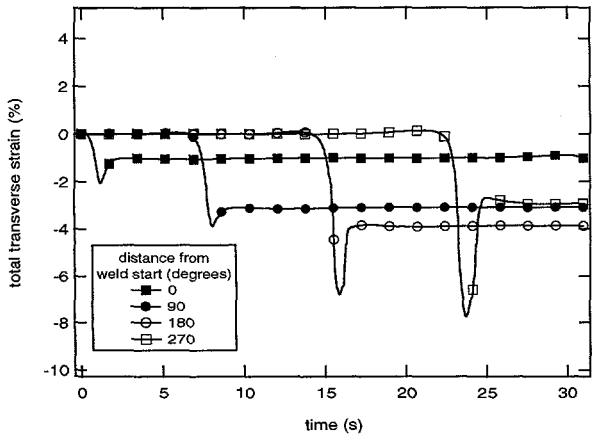

Figure 5. Total transverse strains for elements along disk weld centerline for simulation of Test 2 in Table1.

strains required to cause cracking in several types of solidification cracking susceptibility specimens. They measured the critical strains as functions of temperature and strain rate to develop ductility curves. A schematic of a ductility curve is shown in Figure 7. Matsuda et al. observed that the critical strain typically decreased as the mechanical strain rate was increased. Figure 7 also illustrates a theory by which cracking is determined to occur by comparing the material's ductility curve to calculated or measured mechanical strains, or hot strains as termed in [1]. If the strains are below the ductility curve for all temperatures in the solidification temperature range, the material will not crack (curve 3 in Fig. 7).

Table 2 lists calculated mechanical strains for elements at 0°, 90°, 180°, and 270° for disk tests 1 and 2, as well as for rectangular specimen tests at 55 A and 70 A at

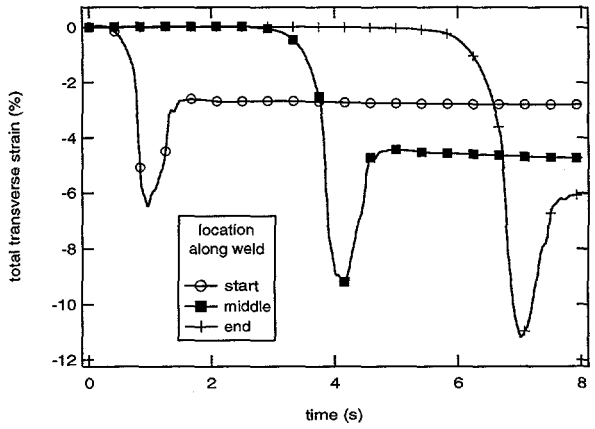

Figure 6. Total transverse strains for elements along rectangular specimen weld centerline for 70 A, 17 V, 12.7 mm/s GTA weld.

the start, midpoint, and near the end of the welds. The mechanical strains listed are calculated at the solidus temperature during solidification. The results for disk tests 1 and 2 show monotonically increasing mechanical strains with distance from the weld start, even though

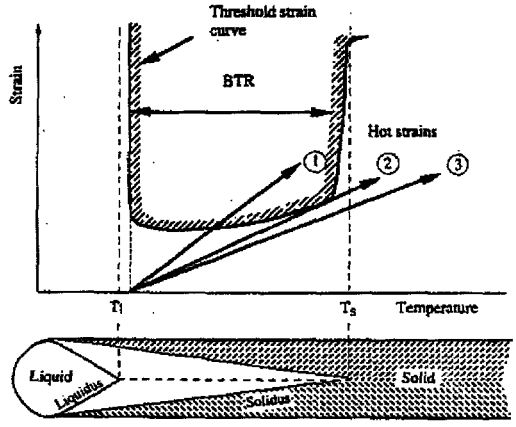

Figure 7. Schematic illustrating concept of hot strain versus threshold strain for predicting solidification cracking, from [1]. Cracking would occur for curve 1. Cracking would not occur for curve 3.

the total strains do not increase monotonically. Mechanical strains in the rectangular plate welds increase with distance from the weld start to beyond the middle of the weld length, then decrease.

Mechanical strains of 3.6% were calculated for the locations where cracks initiated in both the disk tests (0 ° for Test 1, 190 ° for Test 2). Mechanical strains of more than 4% at the solidus temperature were calculated for the 70 A weld, but no cracking was observed in either the 55 A or 70 A rectangular welds. Mechanical strain rates averaged over the solidification temperature range were similar for both specimens (~ 10% s^{-1}) at all locations, indicating that a theory like that illustrated in Figure 7 would suggest that at least the 70 A rectangular plate weld should crack.

Table 2. Calculated mechanical strains accumulated during solidification at various locations for disk and rectangular specimens.

specimen	test	accumulated mechanical strain between liquidus and solidus temperature (%)			
		location			
		0°	90°	180°	270°
disk	1	3.6	3.9	4.1	4.2
disk	2	1.9	2.7	3.6	3.9
		location			
		start	middle		end
rectangular	55A	3.3	3.4		3.1
rectangular	70A	4.0	4.1		3.4

Reference [7] discusses the application of a void-growth based failure model which correctly predicts the location at which continuous cracks form in the disk specimens, and predicts no continuous cracks in the rectangular specimens. The calculations used a strain rate and temperature dependent constitutive model coupled with a void growth damage model. Damage evolution is based on the level of stress triaxiality [9].

6. Summary and Conclusions

Finite element simulations of weld solidification cracking susceptibility tests were presented for two types of specimens. Strain histories for elements on the weld centerline at several locations along the lengths of the welds were examined. Mechanical strains were calculated and compared for different tests and different cracking responses. The comparisons indicate that a strain-based failure criterion would not correctly predict the observed cracking trends for the different specimens. However, there is considerable uncertainty in some aspects of the high temperature material properties. Experimental measurements of strains and temperatures along the weld centerline on different types of specimen are required to more rigorously determine the accuracy of the current models and to address the applicability of strain based and void growth based failure criteria.

7. Acknowledgments

The many weld experiments performed by J. Krafcik are greatly appreciated. This work was funded by the U.S. Department of Energy under contract No. DE-AC04-94AL85000.

References

1 Feng, Z.,"A Methodology for Quantifying the Thermal and Mechanical Conditions for Weld Solidification Cracking", Ph.D. Dissertation, Ohio State University, 1993.

2 Brooks, J. A., Dike, J. J., and Krafcik, J. S., "On Modeling Weld Solidification Cracking", Proc. Modeling and Control of Joining Processes, Orlando, FL, Dec. 1993, ed. T. Zacharia, AWS, 174-185.

3 Feng, Z., and Tsai, C. L., "Modeling the Thermomechanical Conditions at Weld Pool", Proc. Modeling and Control of Joining Processes, Orlando, FL, Dec. 1993, ed. T. Zacharia, AWS, 525-532.

4 Zacharia, T., and Aramayo, G. A., "Modeling of Thermal Stresses in Welds", Proc. Modeling and Control of Joining Processes, Orlando, FL, Dec. 1993, ed. T. Zacharia, AWS, 533-540.

5 Dike, J. J., Brooks, J. A., and Krafcik, J. S., "Finite Element Modeling and Verification of Thermal-Mechanical Behavior in the Weld Pool Region", Proc. 4th International Conference on Trends in Welding Research, Gatlinburg, TN, June, 1995, Ed. H. B. Smartt, J. A. Johnson, S. A. David, 159-164.

6 Feng, Z., Zacharia, T., and David, S. A., "Modeling of Thermomechanical Conditions in the Sigmajig Weldability Test", Proc. 4th International Conference on Trends in Welding Research, Gatlinburg, TN, June, 1995, Ed. H. B. Smartt, J. A. Johnson, S. A. David, 621-626.

7 Dike, J. J., Brooks, J. A., Bammann, D. J., and Li, M., "Thermal-Mechanical Modeling and Experimental Validation of Weld Solidification Cracking in 6061-T6 Aluminum", Proc. of ASM Int'l European Conf. on Welding and Joining Science and Technology, Madrid, Spain, March 10-12, 1997.

8 Nedreberg, M. L., "Thermal Stress and Hot Tearing during the DC Casting of Al-Mg-Si Billets", Ph.D. Dissertation, University of Oslo, 1991.

9 Bammann, D. J., Chiesa, M. L., Horstemeyer, M. F., and Weingarten, L., "Failure in Ductile Materials Using Finite Element Methods", in Structural Crashworthiness and Failure, Jones, N. and Wierzbicki, T.. eds, Elsevier Science Publishers, 1993.

10 Matsuda, F., Nakagawa, H., Nakata, K., Kohmoto, H., and Honda, Y., "Quantitative Evaluation of Solidification Brittleness of Weld Metal during Solidification by Means of In-Situ Observation and Measurement (Report I) - Development of the MISO Technique", 1983, Trans. of JWRI, 12 (1), 65-72.

11 Arata, Y., Matsuda, F., Nakata, K., Shinozaki, K., "Solidification Crack Susceptibility of Aluminum Alloy Weld Metals (Report II) - Effect of Straining Rate on Cracking Threshold in Weld Metal during Solidification", 1977, Trans. of JWRI, 6 (1), 91-104.